Photophysics and Electron Dynamics in Dye-Sensitized Semiconductor Film Studied by Time-Resolved Mid-IR Spectroscopy

Kan Takeshita* and Yutaka Sasaki

Center for Analytical Chemistry and Science, Inc., 1000 Kamoshida-cho, Aoba, Yokohama, 227-0033, Japan

Masahiro Kobashi, Yuki Tanaka, and Shuichi Maeda

Science and Technology Research Center, Mitsubishi Chemical Corporation, 1000 Kamoshida-cho, Aoba, Yokohama, 227-8502, Japan

Akira Yamakata, Taka-aki Ishibashi, and Hiroshi Onishi

Surface Chemistry Laboratory, Kanagawa Academy of Science and Technology (KAST), KSP East 404, 3-2-1 Sakado, Takatsu, Kawasaki 213-0012, Japan

Photophysics and electron dynamics in dye-sensitized semiconductor film were studied by transient mid-IR spectroscopy, in particular on the nano- to millisecond time scale. As sensitizers, a Ru complex and 9-phynol xanthane derivatives were used. We simultaneously observed electrons injected into the conduction band of a semiconductor and the change of vibration bands due to formation of a cation of a dye molecule. The transient absorption components derived from these two species decayed differently. From this observation, we found that injected electrons decay through two paths; one was back electron transfer, and the other was decay to deep trap sites that cannot be detected by mid-IR light. We could also estimate the amount of electron injection for different dye-sensitized TiO_2. Our transient mid-IR spectroscopy in long time scale introduces a semi-new approach to the slow dynamics in dye-sensitized semiconductors including back electron transfer.

1. Introduction

There has been considerable interest in studying the kinetics and mechanism of photoinduced electron transfer for molecules adsorbed on the surface of semiconductor particles.[1−3] This interest is mainly due to the potential use of these systems in solar energy conversion.[3,4] It is important to elucidate electronic processes in these systems, not only for scientific interest but also to obtain information for the design of efficient molecular sensitizers.

In these systems, wide-band gap semiconductors can be sensitized to visible light by the adsorption of dyes on their surface. If the electronic excited state of the sensitizing dye lies, in terms of energy, above the conduction band edge of the semiconductor, electron injection to the conduction band occurs. It is known that the injection of photogenerated electrons into the semiconductor conduction band occurs on the femtosecond time scale,[5−9] which is much faster than the deactivation rate of the excited state to the ground state of the dye. This results in high photon-to-current conversion efficiency.

Furthermore, postinjection processes (e.g., diffusion,[10−12] trapping,[11] and back electron transfer[12−15]) can be important factors that determine photon-to-current conversion efficiency. For example, in a solar cell device the injected electrons diffuse to the collecting back contact, which competes with back electron transfer (recombination) to a dye or redox species in the electrolyte solution. This means that slow back electron transfer can contribute to high photon-to-current conversion efficiency. Therefore, it is essential to understand the factors that determine the rate of back electron transfer. However, these factors have not yet been clarified, and even more importantly, the processes an electron experiences in the semiconductor after injection are not yet completely understood.

Time-resolved mid-infrared absorption spectroscopy is a powerful technique for investigating electron dynamics because it can directly detect injected electrons. There are several studies on dye-sensitized semiconductors by time-resolved mid-IR absorption,[7−9] and these studies have revealed the electron injection rate from the excited state of dye to the semiconductor conduction band. These studies also revealed transient vibrational absorption of adsorbates, which means we can simultaneously monitor substrates and adsorbates by mid-IR light. As mentioned above, relatively slow electron dynamics after injection are also important, but hardly any of these studies observed the postinjection process because the measurement range was of subpicosecond to a few nanoseconds' duration. The usual method for observing these slow electron dynamics has been by measuring bleach recovery of sensitizing dyes with transient absorption in the visible light range.[13,14,16] Although these studies have revealed the back electron transfer rate to dyes or redoxes, there are other electron processes in semiconductors, apart from back electron transfer, such as diffusion or relaxation to shallow and deep traps. Direct observation of injected electrons is absolutely necessary to clarify these electron processes.

* To whom correspondence should be addressed. E-mail: 5503103@cc.m-kagaku.co.jp. Phone: +81−45−963−3155. Fax: +81−45−963−4261.
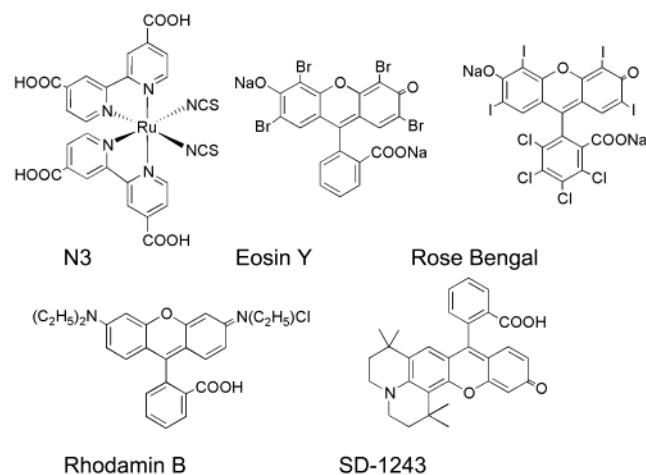
Photophysics in Dye-Sensitized Semiconductor Film

J. Phys. Chem. B, Vol. 107, No. 17, 2003 **4157**

Figure 1. The molecular structures of sensitizing dyes used in this study.

Figure 2. The transient absorption spectra of naked TiO_2 (dotted line) at 5 μs after 355 nm pulse laser excitation and N3-sensitized TiO_2 (solid line) at 5 μs after 532 nm pulse laser excitation. The two signals are normalized at 2200 cm^{-1}. The ground-state spectrum of N3-sensitized TiO_2 is also shown (thin line).

Recently, some authors have developed the systems that can detect transient absorbance changes as small as 10^{-6} over a wide wavenumber range (900−4000 cm^{-1}) and also over a wide range of delay times (50 ns to 1 s).[17,18] These sensitive systems enabled us to detect injected electrons over a long time scale. Here we report the transient mid-IR absorption study for dye-sensitized semiconductor film on a time scale from tens of nanoseconds to a millisecond. We succeeded in the simultaneous observation of the electrons injected into the conduction band and a vibration band change of a sensitizing dye in a long-time scale.

2. Experimental Section

2.1 Sample Preparation. The samples used in this study were dye-sensitized nanocrystalline TiO_2 (or SiO_2 as reference) films. These films were prepared by the procedure reported previously.[19] We used method B described in that literature. Briefly, a TiO_2 colloid solution was made from TiO_2 (P25 Degussa), water, and small amounts of acetylacetone and detergent (Triton X-100). The colloid solution was spread on a CaF_2 plate substrate with a glass rod. After the sample was air-dried, the plate was fired for 30 min at 400 C° in air. Coating of the TiO_2 surface with dye was carried out by soaking the film for 1−3 h in a butanol/acetonitrile dye solution. The reference dye-sensitized SiO_2 (AEROSIL 300) films were prepared in the same way as TiO_2 films. The sensitizing dyes used in this study were ruthenium complex N3; $Ru(dcbpy)_2(NCS)_2$ [dcbpy = (4,4′-dicarboxy-2,2′-bipyridine)]. We also used 9-phynol xanthane derivatives listed in Figure 1. It is known that, among organic dyes, 9-phynol xanthane derivatives show a relatively high photon-to-current efficiency but that they are not comparable to ruthenium complexes such as N3.[20,21] Therefore, a comparison between N3 and these organic dyes is expected to give useful information on the electron dynamics in this system. For the comparison of photon-to-current efficiencies among different dyes, each film sample was prepared as it had roughly the same absorbance at the excitation wavelength.

2.2. Time-Resolved IR Absorption. The detail of the experimental setup for time-resolved infrared absorption is shown elsewhere.[17,18] We used the second harmonic of Q-switched Nd:YAG laser as an excitation pulse (532 nm, 10 ns pulse). The excitation pulse energy was below 0.5−1 mJ/cm², and the repetition rate was 5 Hz. A probe light (emitted from the $MoSi_2$ source) was focused on the sample plate with an ellipsoidal mirror. The transmitted light was dispersed in a
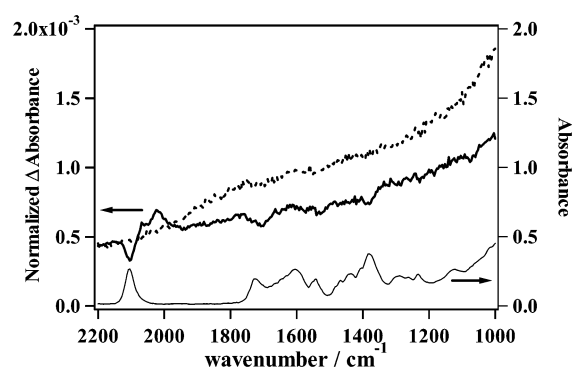
monochromator of 50 cm focal length and the monochromatic output was detected by an MCT (mercury−cadmium−telluride) detector. The MCT output was amplified in AC-coupled amplifiers and accumulated in a digital sampling oscilloscope (Lecroy, LT342L) as a function of delay time at a fixed wavelength. The temporal profiles were reconstructed to transient IR absorption spectra at different delay times. The time-resolution was about 50 ns, which was determined by the response of the detector.

3. Results and Discussion

3.1. N3-Sensitized TiO_2 Film. Since the Grätzel group invented a high performance solar cell using N3-sensitized TiO_2 film,[4,19] this system has become one "standard" for the various studies in this field. In this study, we first applied our time-resolved IR technique to N3-sensitized TiO_2.

Figure 2 shows the transient IR absorption spectra of N3-sensitized TiO_2 and naked TiO_2 after photoexcitation at 532 nm (for N3-sensitized TiO_2) or 355 nm (for naked TiO_2). There was broad and unstructured absorption over the range measured. This broad absorption is ascribed to photogenerated electrons in TiO_2.[18] In naked TiO_2, the electrons are directly excited from valence band to conduction band, while the electrons are injected from the LUMO of the sensitizing dyes to the conduction band of the semiconductor in the case of N3-sensitized TiO_2. In addition to this broad absorption, we can also see a peak and a dip around 2100 cm^{-1} in the spectrum of N3-sensitized TiO_2. We can ascribe this peak and dip to vibration band change of C−N in the NCS ligand. (When an electron of N3 transfers to a semiconductor particle, N3 forms a cation, which means that the Ru(II) metal center becomes Ru(III). Because the Ru(III) metal center has a small electron charge density, it favors the more negatively charged N atom of the NCS ligand. This leads to weakened C−N bond strength and C−N stretch band is shifted to lower energy.[8]) Therefore, this transient absorption spectrum of N3-sensitized TiO_2 includes information on electrons in *both semiconductors and dyes* in one spectrum.

Figure 3 depicts the temporal profile of transient absorption probed at 1950 cm^{-1} of N3-sensitized TiO_2 and SiO_2. We observed strong absorption in N3-sensitized TiO_2 but observed no signal, except a small one originating from photothermal effect in N3-sensitized SiO_2.[23] This observation also supports our assignment of the transient absorption to photogenerated electrons in TiO_2. The electrons excited to the LUMO of dye by visible pulse are injected to the conduction band of the semiconductor in TiO_2, but electron injection cannot occur in
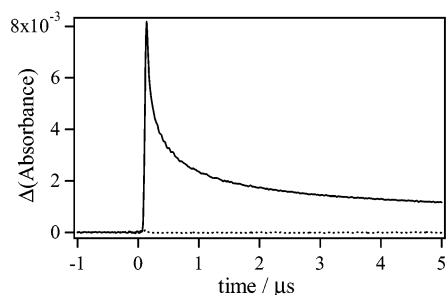
Figure 3. The transient absorption probed at 1950 cm^{-1} of N3-sensitized TiO$_2$ and SiO$_2$ after the excitation by 532 nm laser pulse; solid line TiO$_2$, dotted line SiO$_2$.
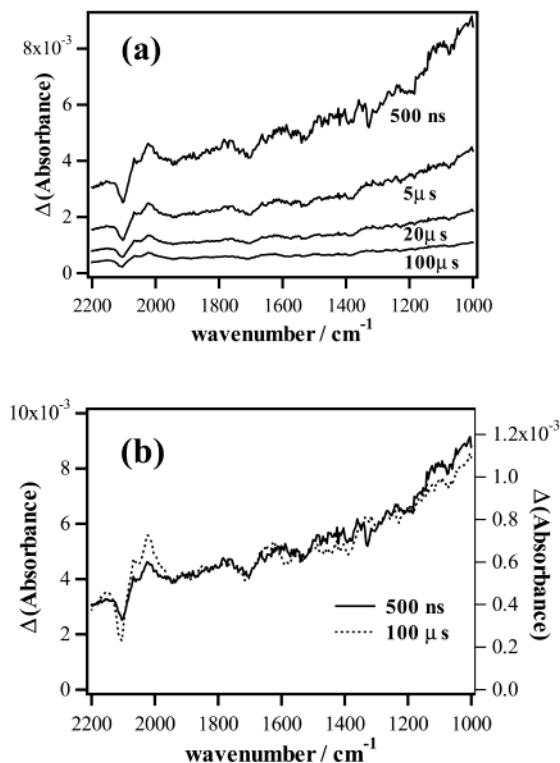

Figure 4. (a) The time evolution of the IR absorption spectrum of N3-sensitized TiO$_2$. (b) The comparison of the spectra between 500 ns (solid line; the intensity is indicated in the left axis) and 100 μs (dotted line; the intensity is indicated in the right axis) after the pulse excitation.

SiO$_2$ because the edge of the conduction band of SiO$_2$ is located at higher than the LUMO of N3.[24] We also show the time evolution of the IR absorption spectrum in Figure 4. The shape of spectrum did not change with the passage of time except the peak and the dip around 2100 cm^{-1}. This observation indicates that the transient absorption due to photogenerated electrons in TiO$_2$ decays in almost the same manner in this wavenumber region.

From the detailed analysis of the temporal change of the N3-sensitized TiO$_2$ spectrum shown in Figure 2, we found that the decay profile at the peak top wavenumber (2025 cm^{-1}) was slightly different from that seen at the other wavenumbers where we observed no peak or dip. Figure 5 shows the decay profile of the transient absorption at 2025 cm^{-1} (A) and 1950 cm^{-1} (B) (Here 1950 cm^{-1} means a wavenumber for which we observed no peak or dip.) This decay difference can be explained by the fact that the absorption at 2025 cm^{-1} includes the contribution from both the injected electrons and the C−N stretch band of the N3 cation, while the absorption at 1950 cm^{-1} has the contribution only from the injected electrons. Here we
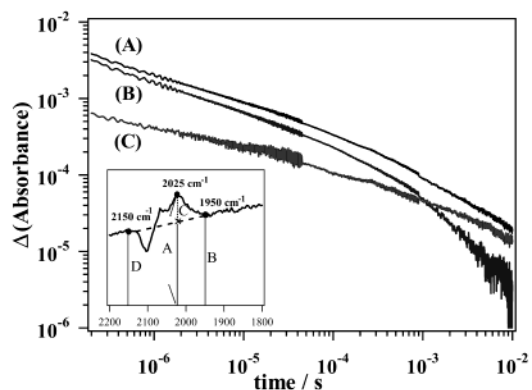

Figure 5. The comparison of the decay profile of the transient absorption at 2025 cm^{-1} (A) with that at 1950 cm^{-1} (B). The inset shows the transient absorption spectrum around 2000 cm^{-1} in the expanded scale. These two decay profiles are slightly different because the absorption at 2025 cm^{-1} is ascribed to the sum of injected electrons and C−N stretch band of N3 cation, while the absorption at 1950 cm^{-1} is ascribed only to injected electrons. Eliminating the injected electron component from line A, we obtain line C, which shows the absorption decay of N3 cation C−N band.

try to separate the transient absorption at 2025 cm^{-1} into two components: "injected electrons" and "N3 cation C−N band". We can estimate the former component from the drawing shown in the inset of Figure 5. We can calculate the "injected electrons" component at 2025 cm^{-1} from the weighted average of the transient absorption at 1950 cm^{-1} (B) and 2150 cm^{-1} (D). By subtracting the "injected electron" component from the total transient absorption at 2025 cm^{-1}, we obtain the "N3 cation C−N band" component, which is shown as line C in Figure 5.

The slope of line C is slightly gentler than that of line B. We interpret this fact as follows. The absorption of the N3 cation C−N band disappears only when the injected electrons go back to N3, but the absorption of injected electrons also disappears through the relaxation to the other sites in the semiconductor that cannot be detected by mid-IR light. That is, the injected electrons have two decay paths leading to the disappearance of absorption (back electron transfer + decay to the other sites in semiconductor), while the N3 cation has only one decay path (back electron transfer).

Electrons injected into semiconductors initially exist in the conduction band. Then they decay to trap sites or go back to N3 dye. If electrons stay in the conduction band or shallow trap sites, they give absorption in the mid-IR region.[18] However, once electrons decay into trap sites that are deep in terms of energy, they give smaller or no absorption in the mid-IR region even though they still exist in the semiconductor. Of course, we cannot eliminate the possibility that some trap sites whose energy levels are not so far from the conduction band edge do not have absorption. However, in our experiment, we call the trap sites that cannot be detected by mid-IR light "deep traps" hereafter, even if they are not deep in terms of energy.

With regard to the mid-IR absorption of electron in deep traps, we have to consider the following two possibilities. One possibility is that electrons in deep traps have *some* absorption in the mid-IR, and this absorption becomes smaller when electrons decay to deeper trap. Another possibility is that electrons in deep traps have *no* absorption in the mid-IR. In the former case, the absorption spectrum due to electrons in deep traps must show a different shape in 2200−1000 cm^{-1} from due to electrons in shallow traps. If that is true, the shape of absorption spectrum in this region will change with the time

Photophysics in Dye-Sensitized Semiconductor Film

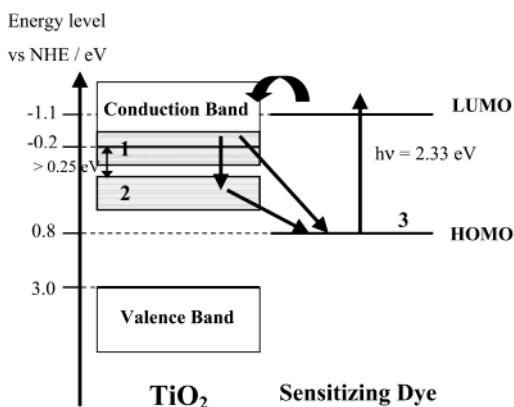*J. Phys. Chem. B, Vol. 107, No. 17, 2003* **4159**

Figure 6. The three states model we use to represent the dynamics of electrons in this system. Each state means conduction band or shallow traps of semiconductor (1), deep traps of semiconductor which cannot be detected by IR light under 2200 cm^{-1} (2), and HOMO of dye molecules (electron which are back to dye molecules) (3). The arrows show the electron flows.

delay. As shown in Figure 4, however, there were no substantial changes in the shape of the transient absorption spectrum in this region. This observation indicates the latter possibility may explain our results better. Therefore, we now assume that deep traps (or a series of deep traps) are energetically separated from the shallow traps and do not give absorption in the region of 2200−1000 cm^{-1}.

Here, we propose a simple model to consider the electron dynamics in this system. In this model, we assume that electrons in the conduction band and shallow traps have the constant absorption cross section for the 2200−1000 cm^{-1} IR light, and that electrons have zero absorption cross section once they decay to deep traps. Under this model, each electron exists in one of the following three states after injection to the conduction band of the semiconductor. (See Figure 6.)

(i) Conduction band or shallow traps of the semiconductor, which can be detected by mid-IR light

(ii) Deep traps of the semiconductor, which cannot be detected by IR light longer than 2200 cm^{-1}

(iii) HOMO of dye molecules (electrons that have reverted to dye molecules)

Although this model is a rough approximation, we can calculate the population ratio of electrons in each state as a function of time based on this model. We define $e_1(t)$, $e_2(t)$, and $e_3(t)$ as normalized population (occupation ratio) in each state at time t, respectively ($e_1(t) + e_2(t) + e_3(t) = 1$). We also assume all electrons exist in state 1 at time 0, i.e., $e_1(0) = 1$. The temporal magnitude of line C in Figure 5 should be proportional to $1 - e_3(t)$, that is, $e_1(t) + e_2(t)$. Also, line B should be proportional to $e_1(t)$. Therefore, by normalizing lines B and C at $t = 0$ and subtracting line B from line C, we can obtain $e_2(t)$. $e_3(t)$ is also calculated from $e_3(t) = 1 - e_1(t) - e_2(t)$. Now we have the population of all three states as functions of time.

Figure 7 shows $e_1(t)$, $e_2(t)$, and $e_3(t)$ − the time profile of electron transition. Just after photoexcitation, almost all electrons exist in the conduction band or shallow traps, and then these electrons decay nonexponentially to deep traps or HOMO of dyes. The electrons that fall into deep traps gradually decay to HOMO of dye. Quantitative analysis of $e_2(t)$ is difficult because the growth and decay of the population of deep traps are complicated processes; decay from the upper state and decay to the lower state. Although we cannot show the quantitative time constant, we conclude that the population of deep traps reaches its maximum at 10^{-5}−10^{-4} second after photoexcitation.
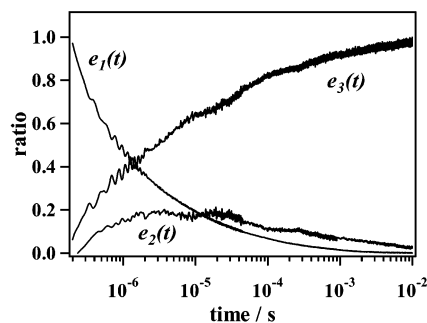

Figure 7. The temporal profile of electron transition: $e_1(t)$, $e_2(t)$, and $e_3(t)$ are the functions of time t which represent normalized population (occupation ratio) in each state shown in Figure 6.

If these deep traps cannot be detected by mid-IR light for energy reasons, the energy levels are lower than the conduction band by more than 0.25 eV. This is because they do not absorb light with a wavelength of less than 2200 cm^{-1} (= 0.27 eV). This 0.25 eV gap significantly affects the efficiency of the cell because the maximum voltage we can extract from N3-sensitized TiO$_2$ type cells is only about 0.7 V.[4,22,25] Furthermore, there is a possibility that the electrons that fall into deep traps never move out to an external circuit and that the only path after falling is back electron transfer to dyes or redox species. These facts mean that the photon-to-current efficiency is hampered by the existence of deep traps in the semiconductor, and that reduction of these traps may improve photon-to-current efficiency. In fact, particle synthesis methods and annealing temperature are expected to change the trap site distribution and density;[26] therefore, we are now conducting an experiment to examine the annealing temperature effect on the IR spectrum. In any case, the investigation of electrons falling into deep traps can give indispensable information for the development of this type of cell.

3.2. 9-Phynol Xanthane Derivatives-Sensitized TiO$_2$ Film. In the previous section, we showed the time-resolved mid-IR absorption technique was powerful to investigate the slow electron dynamics including back electron transfer. In this section, we show this technique is also useful to evaluate the amount of electrons that are injected to the semiconductor, and that this amount is strongly related to the photon-to-current conversion efficiency.

It is known that, as well as metal complexes such as N3, some organic dyes can sensitize semiconductors with relatively high photon-to-current conversion efficiency. In particular, 9-phynol xanthane derivatives show high conversion efficiency.[20,21] However, conversion efficiency is considerably different among these sensitizing dyes. Time-resolved IR spectroscopy can be very helpful in elucidating the reasons for these differences because it can evaluate the quantity of electrons that are injected to the semiconductor and can also investigate slow dynamics including back electron transfer.

We measured transient absorption of TiO$_2$ sensitized by dyes listed in Figure 1 at 1950 cm^{-1} (Figure 8). The excitation pulse energy and other experimental conditions were the same in the different samples. The decay of the transient absorption was slightly different among the different dyes, but the difference was too small to explain the pretty large difference in photon-to-current conversion efficiency. It was rather surprising that Ru complex N3 and organic dyes showed roughly similar decay regardless of their major differences in photon-to-current conversion efficiency. The signal decay contains the information about the postinjection process as pointed out in the previous section. In our case, therefore, the postinjection process (back
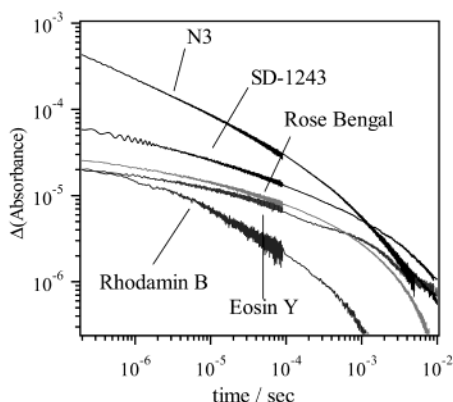
Figure 8. The decay of transient absorption probed at 1950 cm^{-1} of N3, eosin Y, EN121, rhodamin B, and rose bengal-sensitized TiO$_2$ films.

TABLE 1: Absorption Maxima, Fluorescence Lifetimes, and Transient Absorption Intensities for the Sensitizing Dyes Used in This Study[a]

	N3	EosinY	Rose Bengal	rhodamin B	SD-1243
IPCE at λ_{max} for TiO$_2$	75	11[21]	3.5	8[21]	24
absorption λ_{max} (nm)	538	525	585	560	535
fluorescence lifetime	50 ns[32]	3.2 ns	800 ps	1.5 ns	6.0 ns
initial transient absorption intensity at 1950 cm^{-1} (ΔABS/10^{-3})	6.2	0.35	0.41	0.30	0.82

[a] The IPCE (incident photon to current efficiency) values are also shown as a reference.[33] Some of the values in this table were taken from the literatures, the others were measured by our own experiments.

electron transfer and decay to deep traps) does not contribute to overall efficiency very much. On the other hand, the initial intensity of the transient absorption had a rather good relation to the efficiency. The initial intensity of the signal is shown in Table 1 with other features of dyes. N3 gave by far the strongest absorption, and 9-phynol xanthane derivatives gave the transient absorption in the following order: SD-1243 > Rose Bengal > EosinY > Rhodamin B. This order and the relative intensity agree with those of photon-to-conversion efficiency except Rose Bengal. Since the initial intensity of transient absorption reflects the quantity of electron injection, we can say that the conversion efficiency is mostly determined by the initial injection in this case.

As shown in Table 1, all dyes used in this study have strong absorption around excitation wavelength (532 nm). We prepared the sample films with different dyes as they had approximately the same absorbance at 532 nm. Therefore, the amount of photon absorbed by dyes is adequate and almost the same, which means that this factor does not influence solar cell efficiency very much at this time. All dyes used have much longer S1 lifetime compared with the rates of electron injection, because electron injection usually occurs the in subpico- to picosecond range.[5−9] These facts suggest that the electron injection to semiconductor should be the dominant path with regard to the decay of excited state of sensitizing dye.

From the discussion above, it seems that there are no factors that explain the difference in the amount of injected electrons. However, we have to take one thing into account; does every dye adsorbed on the plate contribute to injection? There is a possibility that some dyes are attached to the surface of TiO$_2$ and absorb the light, but never give rise to injection. Here we call this type of dye "*inactive* dye". In this case, the difference

in the amount of injected electrons may be explained by the "ratio of *inactive* dyes". The existence of *inactive* dye was reported previously.[28,29] It is partly explained by the formation of dye aggregate on the semiconductor surface.[28] It can be also explained by site heterogeneity of semiconductor particles on which dyes adsorb.[30,31] To be exact, each dye has its own injection rate depending on the circumstance. Therefore, it is impossible to assume that there exist only two types of dye; one is *active* (has constant injection rate) and the other is *inactive* (never gives injection). However, in the case of 9-phynol xanthane derivative there must be many dyes that show almost no injection, which we can regard as *inactive*. To increase the ratio of *active* dyes, that is, to decrease *inactive* dyes, is one of the most important factors in improving efficiency as a solar cell.

It was unfortunate that back electron-transfer rate or nature of deep traps did not seem to have a strong relation to solar cell efficiency in our study, but our study does not in the least deny the possibility that these factors have a relation to solar cell efficiency in other systems. Our long time scale transient mid-IR system should be applied to different systems, including different substrates such as ZnO$_2$ and SnO$_2$, or TiO$_2$ annealed at different temperatures. We expect the different distributions of trap sites for different substrates or different annealing temperatures. We may be able to obtain useful information by the comparison between solar cell efficiency and electron dynamics in these systems which have the different distributions of trap sites.

4. Summary

Using the time-resolved mid-IR technique for N3-sensitized TiO$_2$, we observed electrons injected into the conduction band of TiO$_2$ and the change of vibration bands due to formation of a radical cation of a dye molecule at the same time. The injected electrons slowly reverted to dye-cation or decayed to deep trap sites that could not be detected by mid-IR light. These deep traps have a strong relation to electronic processes in semiconductor and photon-to-current conversion efficiency.

We could also investigate electron dynamics for TiO$_2$ sensitized by 9-phynol xanthane derivatives. We found that the conversion efficiency was mostly determined by the initial injection. The considerably large difference in the amount of the initial injection may be attributed mostly to the ratio of active dyes which are effective for electron injection.

References and Notes

(1) Gerischer, H.; Michel-Beyerle, M. E.; Rebentrost, F.; Tributsch, H. *Electrochim. Acta* **1968**, *13*, 1509.
(2) Gerischer, H. *Photochem. Photobiol.* **1972**, *16*, 243.
(3) Hagfeldt, A.; Grätzel, M. *Chem. Rev.* **1995**, *95*, 49.
(4) O'Regan, B.; Grätzel, M. *Nature* **1991**, *353*, 737.
(5) Tachibana, Y.; Moser, J. E.; Grätzel, M.; Klug, D. R.; Durrant, J. R. *J. Phys. Chem.* **1996**, *100*, 20056.
(6) Martini, I.; Hodak, J.; Hartland, V. *J. Chem. Phys.* **1997**, *107*, 8064.
(7) (a) Ellingson, R. J.; Asbury, J. B.; Ferrere, S.; Ghosh, H. N.; Sprague, J. R.; Lian, T.; Nozik, A. J. *J. Phys. Chem. B* **1998**, *102*, 6455. (b) Asbury, J. B.; Ellingson, R. J.; Ghosh, H. N.; Ferrere, S.; Nozik, A. J. R.; Lian, T. *J. Phys. Chem. B* **1999**, *103*, 3110. (c) Asbury, J. B.; Hao, E.; Wang, Y.; Ghosh, H. N.; R.; Lian, T. *J. Phys. Chem. B* **2001**, *105*, 4545.
(8) Heimer, T. A.; Heilweil, E. J. *J. Phys. Chem. B* **1997**, *101*, 10990.
(9) Heimer, T. A.; Heilweil, E. J. *Proceedings for Ultrafast Phenomena XI*; Springer-Verlag: Berlin, 1998; pp 505−507.
(10) Schwarzburg, K.; Willing, F. *J. Phys. Chem. B* **1999**, *103*, 5743.
(11) Schwarzburg, K.; Willing, F. *Appl. Phys. Lett.* **1991**, *58*, 2520.
(12) Nelson, J. *Phys. Rev. B* **1999**, *59*, 15374.
(13) O'Regan, B.; Moser, J. E.; Anderson, B.; Grätzel, M. *J. Phys. Chem.* **1990**, *94*, 8720.
(14) Tachibana, Y.; Haque, S. A.; Mercer, I. P.; Durrant, J. R.; Klug, D. R. *J. Phys. Chem. B* **2000**, *104*, 1198.

(15) Salafsky, J. S.; Lubberhuizen, W. H.; van Faassen, E.; Schropp, R. E. I. *J. Phys. Chem. B* **1998**, *102*, 766.

(16) Kuciauskas, D.; Freund, M. S.; Gray, H. B.; Winkler, J. R.; Lewis, N. S. *J. Phys. Chem. B* **2001**, *105*, 392.

(17) Iwata, K.; Hamaguchi. H. *Appl. Spectrosc.* **1990**, *44*, 1431.

(18) (a) Yamakata, A.; Ishibashi, T.; Onishi, H. *Chem. Phys. Lett.* **2001**, *333*, 271. (b) Yamakata, A.; Ishibashi, T.; Onishi, H. *J. Phys. Chem. B* **2001**, *105*, 7258.

(19) Nazeeruddin, M. K.; Kay, A.; Rodicio, I.; Humphry-Baker, R.; Müller, E.; Liska, P.; Vlachopoulos, N.; Grätzel, M. *J. Am. Chem. Soc.* **1993**, *115*, 6382.

(20) Sayama, K.; Sugino, M.; Sugihara, H.; Abe, Y.; Arakawa, H. *Chem. Lett.* **1998**, 753.

(21) Sayama, K.; Arakawa, H. *Shikiso Zokan Taiyo Denchi no Saishin Gijutsu*; Arakawa, H., Ed.; Shi Emu Shi: Tokyo, Japan, 2001; pp 151−159.

(22) Hagfeldt, A. *Sol. Energy Mater. Sol. Cells* **1994**, *31*, 481.

(23) Yuzawa, T.; Kato, C.; George, M. W.; Hamaguchi, H.; Hamaguchi, H.; *Appl. Spectrosc.* **1994**, *48*, 684.

(24) (a) Liu, D.; Kamat, P. V. *J. Chem. Phys.* **1996**, *105*, 965. (b) Martini, I.; Hartland, G. V.; Kamat, P. V. *J. Phys. Chem. B* **1997**, *101*, 4826.

(25) Murakoshi, K.; Yanagida, S. *J. Electroanal. Chem.* **1995**, *396*, 27.

(26) Nakade, S.; Matsuda, M.; Kambe, S.; Saito, Y.; Kitamura, T.; Sakata, T.; Wada, Y.; Mori, H.; Yanagida, S. *J. Phys. Chem. B* **2002**, *106*, 10004.

(27) (a) Cherepy, N. J.; Smestad, G. P.; Grätzel, M.; Zhang, J. Z. *J. Phys. Chem. B* **1997**, *101*, 9342. (b) Heimer, T. A.; Heilweil, E. J.; Bignozzi, C. A.; Meyer, G. J. *J. Phys. Chem. A* **2000**, *104*, 4256.

(28) Barzykin, A, V,; Tachiya, M. *J. Phys. Chem. B* **2002**, *106*, 4356.

(29) Hara, K.; Horiuchi, H.; Katoh, R.; Singh, L. P.; Sugihara, H.; Sayama, K.; Murata, S.; Tachiya, M.; Arakawa, H. *J. Phys. Chem. B* **2002**, *106*, 374.

(30) Katoh, R.; Furube, A.; Hara, K.; Murata, S.; Sugihara, H.; Arakawa, H.; Tachiya, M. *J. Phys. Chem. B* **2002**, *106*, 12957.

(31) Khazraji, A. C.; Hotchandani, S.; Das, S.; Kamat, P. V. *J. Phys. Chem. B* **1999**, *103*, 4693.

(32) Grätzel, M. *Cattech* **1999**, *3*, 4.

(33) The IPCE measurement was not conducted with the same absorbance for different samples, but it was conducted at the absorption maximum for each sample. The absorbance of the sample was high (>1) enough to consider nearly all incident photons are absorbed by the sample at the measurement wavelength. Therefore, the amount of photons absorbed by dyes has little influence on these IPCE values.